

# Characteristics and generation process of surface waves excited on a perfect conductor surface

Fumiaki Miyamaru,<sup>1,2</sup> Mototsugu Kamijyo,<sup>2</sup> Keisuke Takano,<sup>3</sup> Masanori Hangyo,<sup>3</sup>  
Hiroshi Miyazaki,<sup>4</sup> and Mitsuo Wada Takeda<sup>2</sup>

<sup>1</sup>Department of Physics, Faculty of Science, Shinshu University, Matsumoto, Nagano 390-8621, Japan

<sup>2</sup>PRESTO, Japan Science and Technology Agency, Aoba, Sendai 980-8577, Japan

<sup>3</sup>Institute of Laser Engineering, Osaka University, 2-6 Yamadaoka, Suita, Osaka 565-0871, Japan

<sup>4</sup>Department of Applied Physics, Faculty of Engineering, Tohoku University, Aramaki, Aoba, Sendai 980-8579, Japan

\*miyamaru@shinshu-u.ac.jp

**Abstract:** We investigate characteristics and generation process of surface waves excited on a structured perfect conductor surface in order to clarify the mechanism of resonant transmission in metal hole arrays made of the perfect conductor. By using a metal hole array of kagome lattice, we can separate two modes excited on the perfect conductor surface; a surface wave and an edge mode. Our calculation based on finite-difference time-domain method provides a generation process of the edge mode and the surface wave that is responsible for the resonant transmission in metal hole arrays.

©2010 Optical Society of America

OCIS codes: (050.0050) Diffraction and gratings; (160.5298) Photonic crystals.

---

## References and links

1. R. Ulrich, "Far-infrared properties of metallic mesh and its complementary structure," *Infrared Phys.* **7**(1), 37–55 (1967).
2. T. W. Ebbesen, H. J. Lezec, H. F. Ghaemi, T. Thio, and P. A. Wolff, "Extraordinary optical transmission through sub-wavelength hole arrays," *Nature* **391**(6668), 667–669 (1998).
3. M. Sarrazin, and J.-P. Vigneron, "Role of Wood anomalies in optical properties of thin metallic films with a bidimensional array of subwavelength holes," *Phys. Rev. B* **71**, 075404 (2005).
4. F. J. García de Abajo, "Light scattering by particle and hole arrays," *Rev. Mod. Phys.* **79**(4), 1267–1290 (2007).
5. F. Miyamaru, and M. Hangyo, "Finite size effect of transmission property for metal hole arrays in subterahertz region," *Appl. Phys. Lett.* **84**(15), 2742–2744 (2004).
6. J. Bravo-Abad, F. J. García-Vidal, and L. Martín-Moreno, "Resonant transmission of light through finite chains of subwavelength holes in a metallic film," *Phys. Rev. Lett.* **93**(22), 227401 (2004).
7. F. J. García-Vidal, E. Moreno, J. A. Porto, and L. Martín-Moreno, "Transmission of light through a single rectangular hole," *Phys. Rev. Lett.* **95**(10), 103901 (2005).
8. F. Miyamaru, and M. Takeda, "Coupling between localized resonance and excitation of surface waves in metal hole arrays," *Phys. Rev. B* **79**(15), 153405 (2009).
9. J. B. Pendry, L. Martín-Moreno, and F. J. Garcia-Vidal, "Mimicking surface plasmons with structured surfaces," *Science* **305**(5685), 847–848 (2004).
10. F. J. Garcia-Vidal, L. Martín-Moreno, and J. B. Pendry, "Surfaces with holes in them: new plasmonic metamaterials," *J. Opt. A, Pure Appl. Opt.* **7**(2), S97–S101 (2005).
11. P. Lalanne, and J. P. Hugonin, "Interaction between optical nano-objects at metallo-dielectric interfaces," *Nat. Phys.* **2**(8), 551–556 (2006).
12. L. Aigouy, P. Lalanne, J. P. Hugonin, G. Julié, V. Mathet, and M. Mortier, "Near-field analysis of surface waves launched at nanoslit apertures," *Phys. Rev. Lett.* **98**(15), 153902 (2007).
13. H. Liu, and P. Lalanne, "Microscopic theory of the extraordinary optical transmission," *Nature* **452**(7188), 728–731 (2008).
14. E. Moreno, S. G. Rodrigo, S. I. Bozhevolnyi, L. Martín-Moreno, and F. J. García-Vidal, "Guiding and focusing of electromagnetic fields with wedge plasmon polaritons," *Phys. Rev. Lett.* **100**(2), 023901 (2008).
15. G. Veronis, and S. Fan, "Modes of Subwavelength Plasmonic Slot Waveguides," *J. Lightwave Technol.* **25**(9), 2511–2521 (2007).
16. A. Degiron, H. J. Lezec, N. Yamamoto, and T. W. Ebbesen, "Optical transmission properties of a single subwavelength aperture in a real metal," *Opt. Commun.* **239**(1-3), 61–66 (2004).
17. H. Raether, in *Surface Plasmons on Smooth and Rough Surfaces and on Gratings*, (Springer, Berlin, 1988).
18. T. Matsui, A. Agrawal, A. Nahata, and Z. V. Vardeny, "Transmission resonances through aperiodic arrays of subwavelength apertures," *Nature* **446**(7135), 517–521 (2007).
19. F. Miyamaru, M. Tanaka, and M. Hangyo, "Resonant electromagnetic wave transmission through strontium titanate hole arrays with complex surface waves," *Phys. Rev. B* **74**(11), 115117 (2006).

## 1. Introduction

In the last few decades, a considerable number of groups have investigated the resonant transmission properties of electromagnetic waves in metal hole arrays (MHAs). In 1967, Ulrich [1] reported the band-pass transmission characteristics of MHAs and attributed them to the excitation of Zenneck waves in the radio-frequency region. After Ebbesen *et al.* [2] demonstrated that subwavelength MHAs exhibit extraordinary transmission characteristics in the visible region, many studies have been reported to understand the mechanism of resonant transmission [3–8]. The dominant mechanism is attributed to the excitation of the surface plasmon polaritons (SPPs) which are localized at the metal-dielectric interface. However, the fact that the resonant transmission is observed over the broad frequency regions, ranging from the radio-frequency to the visible regions, makes it difficult to understand the mechanism. In the low-frequency region, i.e., below the terahertz (THz) frequency region, metals are regarded as almost perfect conductors where the localization of the SPPs in the vicinity of the metal surface becomes extremely weak, and consequently, the resonant transmission cannot be expected to occur. In order to solve this problem, Pendry proposed an effective theory for the periodically structured metal surface, called a spoof SPP model [9,10]. However, this model is applicable only when the period is much smaller than the wavelength of the electromagnetic wave at the resonant frequency. It is difficult to extend the Spoof SPP model to explain the mechanism of the resonant transmission in MHAs. Lalanne *et al.* [11–13] proposed another model that takes into account the contribution of the surface wave, called a cylindrical wave (CW). This CW can be excited even on a perfect conductor surface [13]. An important achievement of their model [11] is that it can treat the mechanism of resonant transmission for a broad spectral range with a crossover of contributions from two kinds of excited electromagnetic modes, the SPPs and CWs. In the high-frequency regime, such as the visible and near-infrared regions, the contribution of the SPPs is considerably larger than that of the CWs. On the other hand, in the low-frequency regime below the mid-infrared region, the contribution of the CWs is more dominant than that of the SPPs.

Lalanne's model [13] has opened the door for providing a comprehensive explanation of the resonant transmission mechanism over a broad frequency range. However, the detailed characteristics of surface waves (SWs) excited on the perfect conductor have not yet been clarified. In this study, we investigate the characteristics and generation process of SWs for a hole array on a perfect conductor. The SWs can be excited when the incident light is scattered by periodically arranged hole arrays. In this scattering process, the electromagnetic mode, called edge mode in recent studies [14,15], is excited at the hole edge. The physical origin of this edge mode is attributed to the resonating dipole which is similar to the localized surface plasmons [16]. Although the characteristic of the edge mode is similar to that of localized surface plasmons, the edge mode can be excited even if metals are regarded as perfect conductors. It is considered that the energy of the edge mode is transferred to the electromagnetic waves propagating along the surface, and consequently, the SWs are generated. The finite difference time domain (FDTD) method is a good tool for investigating the spatiotemporal distribution of the electric field. However, in a periodical structure such as a triangular lattice (the top figure of Fig. 1a), the edge modes and SWs cannot be distinguished because these two modes are excited at the same position in space; a schematic representation is shown in the bottom figure of Fig. 1a. In order to separate the spatial distributions of these two modes, we use the MHAs of the kagome lattice structure (the top figure of Fig. 1b). By using this structure, we can obtain the spatiotemporal characteristics of these two modes separately in space (see the bottom figure of Fig. 1b), and consequently the underlying physics of the SWs excited on the perfect conductor can be studied.

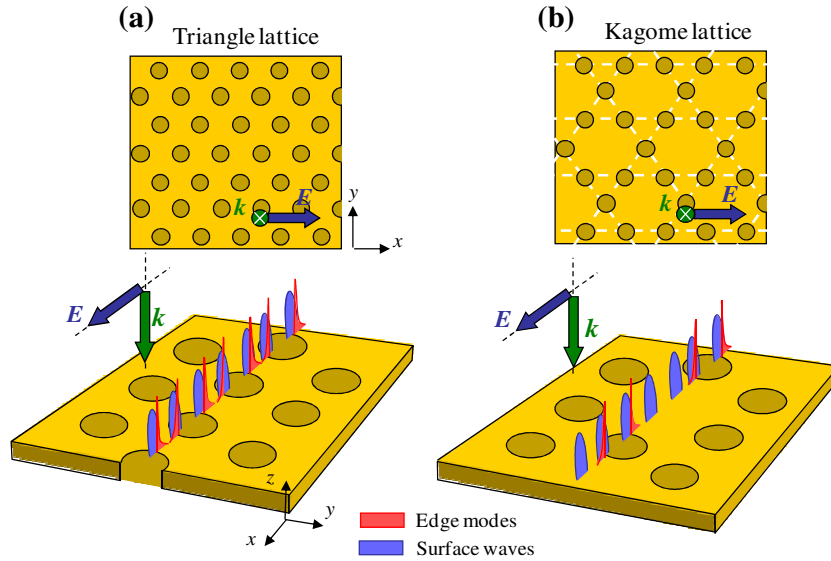


Fig. 1. Schematic representations of metal hole arrays of (a) a triangular lattice and (b) a kagome lattice. The bottom figures show the conceptual diagrams of the electric field distribution of an edge (red area) mode and the SW (blue area) excited on the surface of a structured perfect conductor. The incident polarization and the wave vector are also shown in these figures.

## 2. Experiment and simulation

We have fabricated MHAs on a 250- $\mu\text{m}$ -thick aluminum plate. The metal holes, having a diameter  $d$  of 500  $\mu\text{m}$ , are arranged in a triangular lattice structure with the periodicity  $a = 1000 \mu\text{m}$  and a kagome lattice structure. The schematic representations of these samples are shown in the top figures of Figs. 1a and 1b, respectively. The kagome lattice consists of a periodic arrangement of three sets of parallel lines, rotated by  $60^\circ$  with respect to each other (see the white dashed line in Fig. 1b). In our sample, we arrange the metal holes at the cross points of these lines; the distance of the closest holes is  $p = 1000 \mu\text{m}$ , which is the same as Fig. 1a. The transmission spectra of the samples at normal incidence are measured by a THz time-domain spectroscopic (THz-TDS) system that allows us to measure the waveform of the THz wave directly in the time domain. Using a Fourier transformation, we can calculate the transmission and phase spectra from the time-domain waveforms transmitted through the samples and air used as a reference. The electromagnetic properties of the samples are computed using the FDTD approach

## 3. Results and discussion

Figure 2a shows the measured transmission spectra for the MHAs of the triangular lattice (black line) and the kagome lattice (red line) at normal incidence. In the spectrum of the triangular lattice, the transmission peak is observed at 0.32 THz with a transmittance of approximately 28%. The resonant frequency  $f_{\text{SW}}$  of the SW excited on the surface of the periodic structure is calculated from [17]

$$f_{\text{SW}} = |\mathbf{k}_{\text{in}} + \mathbf{G}| \frac{c}{2\pi} \left( \frac{\varepsilon_m + \varepsilon_d}{\varepsilon_m \varepsilon_d} \right)^{1/2}, \quad (1)$$

where  $\mathbf{k}_{\text{in}}$  is the in-plane wave vector of the incident electromagnetic wave,  $\mathbf{G}$  is the reciprocal lattice vector, and  $\varepsilon_m$  and  $\varepsilon_d$  are the dielectric constants of the metal and the attached dielectric (air in the present case), respectively. From Eq. (1), the lowest order of  $f_{\text{SW}}$  is estimated to be

0.34 THz for the MHA ( $\epsilon_m \gg \epsilon_d = 1$ ) at normal incidence ( $|\mathbf{k}_{in} + \mathbf{G}| = \frac{2}{\sqrt{3}} \frac{2\pi}{a} = 7.25 \times 10^3$

$\text{m}^{-1}$ ), which is close to 0.32 THz of experimental result. In the spectrum of the kagome lattice, the transmission peak is observed at the same frequency as in the triangular lattice although the peak transmittance is approximately 7%, which is four times weaker than that of the triangular lattice. This transmission peak indicates that the resonant transmission occurs in the MHAs with the kagome lattice as well as in the triangular lattice. Figure 2b shows the simulated transmission spectra for the same structures as those in Fig. 2a. The resonant transmission peaks are observed in both the triangular lattice and the kagome lattice, in good qualitative agreement with the experiments. These agreements demonstrate the accuracy of the FDTD simulation for our structures.

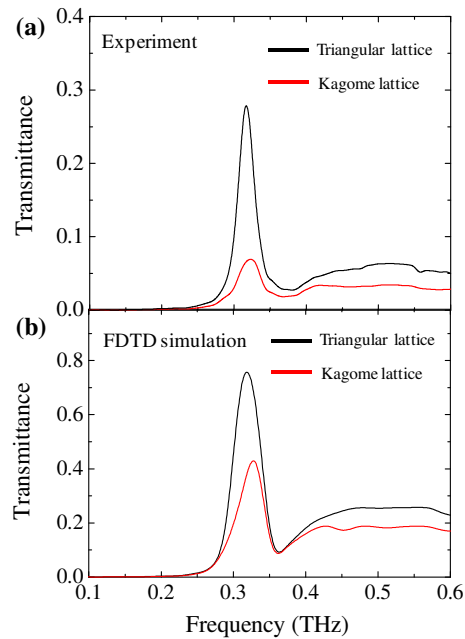


Fig. 2. (a) Measured transmission spectra for the MHAs of the triangular lattice (black line) and the kagome lattice (red line). (b) Simulated transmission spectra for the MHAs of the triangular lattice (black line) and the kagome lattice (red line).

Next, we investigate the steady spatial distribution of the electric field in the vicinity of the metal surfaces. Figures 3a and 3b show the distribution of the  $z$ -component of the electric field  $E_z$  in the  $x$ - $y$  and  $x$ - $z$  planes, respectively, for the MHA of the triangular lattice. Similar distributions for the kagome lattice are shown in Figs. 3c and 3d. For these simulations, the incident electromagnetic wave at the resonant frequency (0.32 THz) impinges at normal incidence. Figures 3a and 3c show the  $x$ - $y$  plane at  $z = 135 \mu\text{m}$ , which is  $10 \mu\text{m}$  above from the illuminated metal surface. Figures 3b and 3d show the  $x$ - $z$  plane at  $y = 0 \mu\text{m}$  as indicated by the dashed lines in Figs. 3a and 3c. All axes are normalized by the lattice constant  $a = 1000 \mu\text{m}$ . For the triangular lattice, a strong localization of  $E_z$  is observed at the edge of the metal holes. Such strong localization of the electric field at the sharp metallic edges is generally observed (we call it “edge mode”) [15] even when the metal is regarded as a perfect conductor [13]. However, the localization of  $E_z$  does not necessarily mean that the SW is excited on the perfect conductor surface. Therefore, it is difficult to provide clear evidence for the excitation of the SWs in the triangular lattice.

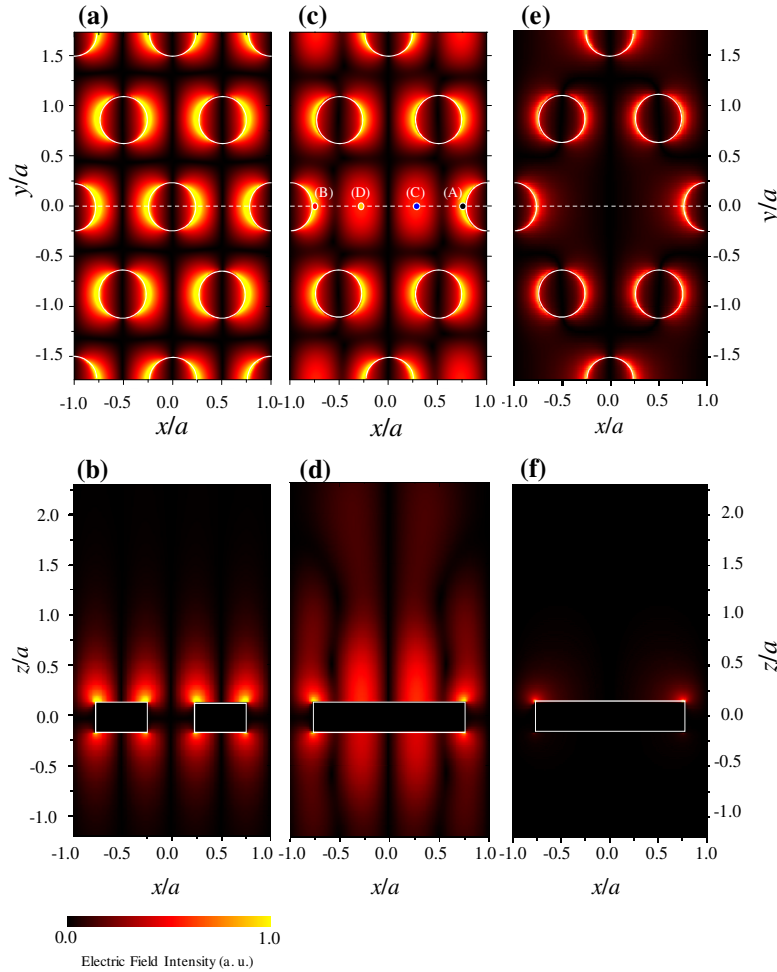


Fig. 3. (a) and (b) Spatial distribution of the  $z$ -component of the electric field  $E_z$  in the  $x$ - $y$  plane at  $z = 135 \mu\text{m}$  and the  $x$ - $z$  plane at  $y = 0 \mu\text{m}$ , respectively, for the MHA of the triangular lattice. The incident electromagnetic wave at the resonant frequency (0.32 THz) impinges at normal incidence. (c) and (d) Same as in (a) and (b) for the MHA of the kagome lattice. (e) and (f) Same as in (c) and (d) except that the frequency of the incident electromagnetic wave is set to the off-resonant frequency (0.1 THz).

On the other hand, in the kagome lattice, the SW is distinguishable from the edge mode. In Figs. 3c and 3d, the localization of  $E_z$  is observed on a flat part of the perfect conductor surface ( $(x/a, y/a) = (\pm 0.25, 0)$ ). Although the attenuation length  $L$  of the SW along the  $z$ -axis is approximately twice as long as that of the edge mode, it is still shorter than the wavelength  $\lambda_{\text{res}}$  at the resonant frequency. For the sake of comparison, we perform the same simulations for the MHA of the kagome lattice at the off-resonant frequency as shown in Figs. 3e and 3f. Although the excitation of the edge mode can be observed even at the off-resonant frequency, the excitation of the SW cannot be observed. These results provide the evidence that the SW is certainly excited on the flat metal surface at the resonant frequency.

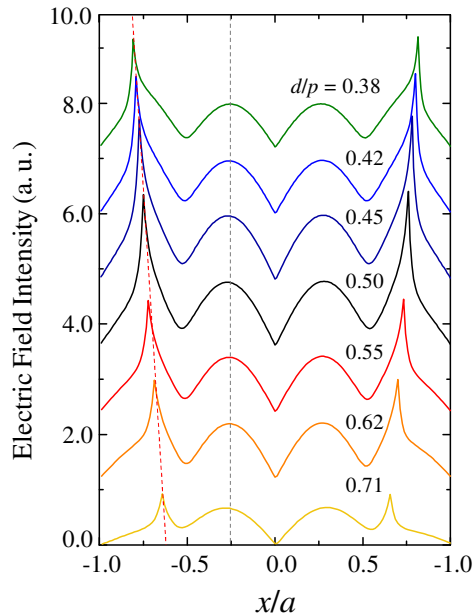


Fig. 4. Spatial distribution of the  $z$ -component of the electric field  $E_z$  along the  $x$ -axis at  $y = 0$   $\mu\text{m}$  and  $z = 135$   $\mu\text{m}$  for various hole diameters  $d$  with respect to the distance of the closest holes  $p$ .

Now, we look into the detailed characteristics and generation mechanism of the SW and edge mode for the MHA of the kagome lattice. There are two important characteristics that should be clarified: (1) the relation between the spatial distributions of the SW and the edge mode in a steady state, and (2) the time evolution of the electric fields of both modes. The former characteristic can be investigated by changing  $d$  with respect to  $p$ . Figure 4 shows the intensity of  $E_z$  as a function of the  $x$  position at  $y = 0$   $\mu\text{m}$  and  $z = 135$   $\mu\text{m}$  for various hole diameters ranging from  $d/p = 0.38$  to  $d/p = 0.71$ . The peak position of the edge mode shifts with  $d/p$  as indicated by the red dashed line. This is expected because the edge mode must be excited at the edge of the metal hole. Contrary to that of the edge mode, the peak position of the SW is almost independent of  $d/p$ , indicating that the spatial distribution of the surface mode is not determined by the hole diameter but by the lattice structure. When we observe the spatial distribution around the edge of the metal hole carefully, it is noticed that the electric field distribution of the SW is superimposed on the distribution of the edge mode. From this result, the total electric field distribution observed in Figs. 3c and 3d can be understood as follows: the SW, whose distribution is determined mainly by the lattice structure, extends over the entire surface of the kagome lattice, and the edge mode that also contributes to the total distribution is localized at the edge of the metal hole. Such an electric field distribution is basically applicable to the MHA of the triangular lattice and, more generally, to the MHAs of other structures, e.g., a square lattice and a quasi-periodical structure [18]. However, in these structures, it is difficult to distinguish the contributions from the two modes because the peak intensities of the two modes are located at almost the same position. Additionally, the fact that the intensity of the edge mode is considerably higher than that of the SW makes the contribution from the SW invisible.

In the previous paragraph, we investigated the spatial distribution of  $E_z$  in the steady state. Here, we investigate the time evolution of the spatial distribution which provides the

understanding of the generation mechanism of the edge mode and SW. Figure 5a shows the time variation of  $E_z$  for the kagome lattice at various positions (indicated by (A)–(D) in Fig. 3c). We use a continuous wave (the frequency  $f = 0.32$  THz) as the incident electromagnetic wave that reaches the metal surface at  $t = 3.5$  ps. From the result of this simulation, the generation process of the SWs is considered to be as follows: At  $t = 3.5$  ps, the electric field localization is observed at the edge of the metal hole (a spatial distribution is shown in Fig. 5b), meaning that only the edge mode is excited. The amplitude around the edge increases with time (black and red lines). The energy of the edge mode transfers to the electromagnetic wave that propagates along the surface gradually, resulting in the excitation of the SW in the flat area at  $t = 6.5$  ps (see blue and yellow lines in Fig. 5a and the electric field distribution in Fig. 5c). At  $t = 12.2$  ps, the excitation of the SW is clearly observed (Fig. 5d), and the amplitudes of both the edge mode and the SW tend to be saturated after  $t = 30$  ps. It is expected that this SW generation process is applicable to the case of the MHAs of the triangular lattice and that the SW can contribute dominantly to the resonant transmission as proposed by Ref. 13. This kind of SW is also applicable to the hole arrays of non-metallic materials. As reported in Ref. 19, the resonant transmission characteristic can be observed even when the real part of the permittivity of the material is very high and positive value. The higher value of the permittivity leads to the larger scattering strength at the edge of holes, and consequently the larger intensity of the SW excitation.

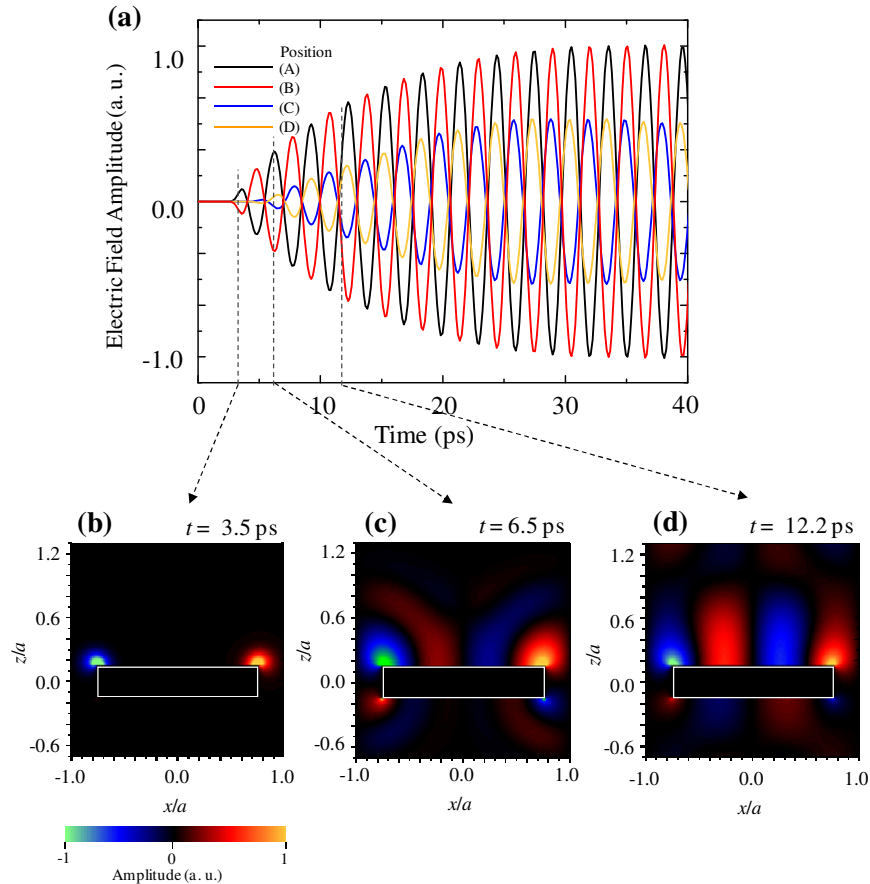


Fig. 5. (a) Time variations of the amplitude of  $E_z$  at various positions (A)–(D) as indicated in Fig. 3(c). (b)–(d) Spatial distributions of the electric field amplitude of  $E_z$  in the  $x$ – $z$  plane at  $y = 0$  mm for various time steps  $t =$  (b) 3.5, (c) 6.5, and (d) 12.2 ps.

#### **4. Summary**

In summary, we have discussed the detailed characteristics and the generation mechanism of the SWs on a structured perfect conductor surface. In the case of the MHA of the perfect conductor, the SWs play a crucial role in the resonant transmission. Our analysis, based on the FDTD method, has provided a detailed understanding of how the SWs are excited. The incident electromagnetic wave excites the edge mode at the edge of the metal holes. This excitation process is a nonresonant process that occurs in a broad frequency range. Then, the energy of the edge mode is transferred to the electromagnetic wave that propagates along the metal surface, resulting in the excitation of the SWs even on the perfect conductor surface. We believe that although our analysis is for SWs on the perfect conductor surface, a similar mechanism is possibly applied to the excitation of the SPPs that take a dominant role in the visible or near-infrared regions.

#### **Acknowledgements**

This work was supported partially by the Ministry of Education, Science, Sports and Culture, Grant-in-Aid for Scientific Research (A) Nos. 20244047 and 20246022, and for Young Scientists (B) No. 21760036.